Video Traffic Management in HSDPA via GEO Satellite

Giovanni Giambene*, Samuele Giannetti*, Cristina Párraga Niebla†, Michal Ries‡

*CNIT – University of Siena, Via Roma, 56, I-53100 Siena, Italy, email: giambene@unisi.it
†DLR – Institute of Communications and Navigation, P.O.Box 11 16, D-82230 Wessling, Germany
‡Institute of Communications and Radio Frequency Engineering, Gusshausstrasse 25/389, A-1040 Vienna, Austria

***Abstract*— This paper investigates video traffic management and packet-scheduling aspects for *Satellite Universal Mobile Telecommunication System* (S-UMTS) transmissions based on *High Speed Downlink Packet Access* via geostationary *Satellite* (S-HSDPA). In particular, this paper surveys resource allocation constraints to be considered for S-HSDPA and investigates the performance of different scheduling schemes in the presence of a GOOD/BAD channel and their influence on the objective video quality for typical UMTS video streaming scenarios. This work has been carried out within the framework of the European SatNEx II network of excellence.**

I. Introduction

High Speed Downlink Packet Access (HSDPA) is a cost-efficient upgrade of current 3G (W-CDMA) systems that delivers performance comparable to today's wireless LAN services, but with the added benefit of mobility. HSDPA's improved spectrum efficiency enables much faster downstream throughput than today's UMTS, giving users downlink speeds typically between 1 - 3 Mbit/s. Hence, capacity-demanding applications are possible, such as video streaming.

Satellite systems are a valid alternative to cover wide areas on the Earth and to provide broadband communications to mobile and fixed users. Satellite systems should be able to provide to mobile users the same access characteristics of the terrestrial counterparts. In such a context, the S-UMTS Family G specification set aims at achieving the satellite air interface fully compatible with W-CDMA-based systems. In this paper, the interest is on the extension of the terrestrial HSDPA to a *geostationary* (GEO)-based satellite network in order to support broadband multimedia applications and, in particular, video streaming and Web downloading for mobile users.

Referring to video streaming, which is the main application considered in this paper, the interest is in using in the satellite context the same video codecs that are employed for terrestrial 3G systems, characterized by low resolutions and low bit-rates. Mobile terminals have limited processing capabilities and power, so the decoding of higher rate videos becomes a quite challenging task. Therefore, the mandatory codec for UMTS streaming applications is H.263 [1], with settings depending on the streaming content type and the streaming application [2]. The used resolutions are *Quarter Common Intermediate Format* (QCIF, 176×144 pixels) for cell-phones, *Common Intermediate Format* (CIF, 352×288 pixels) and *Standard Interchange Format* (SIF, 320×240 pixels) for data-cards and PDAs. It can be assumed that the maximum supported video bit-rates are 105 kbit/s for QCIF resolution and 200 kbit/s for CIF and SIF resolutions. Then, the encoded video stream is encapsulated into 3gp or mp4 file format [3]. Clients and streaming servers shall support an IP-based network interface for the transport of session control and video data by using the RTP/UDP/IP protocol stack (see Fig. 1) [3].

The video streaming services over UMTS/HSDPA in the packet-switched domain suffer from packet losses and delay that depend on radio channel conditions. Packet loss and delay produce various kids of artifacts and their possible spatial and temporal propagation [4].

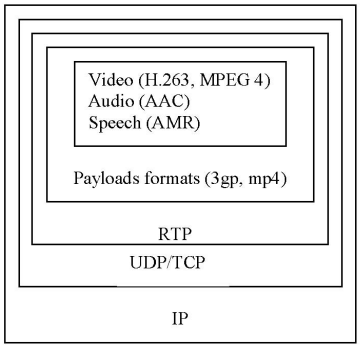

Fig. 1. Overview of the video streaming protocol stack.

II. S-HSDPA Air Interface

HSDPA is based on the application of *Adaptive Code and Modulation* (ACM) and multi-code operation depending on the channel conditions (forward link) that are feed back by the *User Equipment* (UE) [5],[6],[7].

In this paper, a multi-beam GEO bent-pipe satellite is considered. All resource management functions for the S-HSDPA air interface are managed by the base station (i.e., Node B) on the Earth that is directly linked to the *Radio Network Controller* (RNC) that operates as a gateway towards the core network. The RNC commands the UE to report the *Channel Quality Indicator* (CQI) value with a certain periodicity (in our scenario the CQI reporting interval is 40 ms). If CQI indicates that the quality is degrading, the resource

manager in the Node B can choose a less ambitious ACM level, which will cope better with the poor channel conditions.

We consider that the CQI value provides the following information related to the transmission characteristics currently supported by the UE [9],[10]:

- Modulation and coding used (i.e., *Transport Format and Resource Combination*, TFRC, mode);
- Number of parallel codes that can be used by the UE for its transmission;
- Specification of a transport block size (that is the basic data unit exchanged between the transport layer and the physical layer [7]) for which the UE would be able to receive at a low *Frame Error Rate* (FER) value, suitable for the satellite scenario.

A GOOD/BAD channel model has been considered in our S-HSDPA scenario [8]; the sojourn times in GOOD and BAD states are sufficiently long (respectively 6 and 2 s) as compared to the GEO satellite round-trip propagation delay (560 ms) to permit a physical layer adaptation on the basis of the channel state information (i.e., CQI) sent back by the UE. Correspondingly, two CQI values have been employed with corresponding transmission modes (i.e., TFRCs) and related transport block sizes of 3319 bits in the BAD state and of 14411 in the GOOD one.

Due to the significant round-trip propagation delay of the GEO scenario (i.e., 560 ms), there are time intervals during which the transmission is done with an unappropriate TFRC mode for the channel. In particular, in the presence of a transition from BAD to GOOD, for 560 ms the system uses a more conservative mode than necessary and FER = 0. Whereas, in the presence of a transition from GOOD to BAD the transmission for 560 ms is not adequately protected so that we assume FER = 0.1.

Note that the high propagation delay of the GEO satellite scenario practically prevents the use of retransmissions (as in the terrestrial HSDPA) to recover packet losses for real-time traffic. This is the reason why the transmission modes for GOOD and BAD states have to guarantee particularly low FER values. This is a mandatory cross-layer optimization for having an acceptable video streaming quality in our GEO satellite scenario. Hence, when radio channel conditions and TFRC mode are aligned, a very low residual FER of 0.0001 has been assumed.

III. S-HSDPA Schedulers

The resource manager in the Node B is composed of two parts: there is a first block that keeps track of the current transmission modes (on the basis of the CQI values sent back by the UEs) supported by the UEs; there is another block, the *scheduler*, that operates at the MAC level (MAC-hs, in particular) and assigns transmission resources to the UEs, i.e., it selects the UE scheduled in the next *Transmission Time Interval* (TTI) and, supported by the link adaptation functionality, the TFRC and number of assigned codes. The TTI interval is typically of 2 ms for a finer granularity in resource allocation. The scheduler at the MAC-hs level has different queues for the different UEs (downlink transmissions); the scheduler serves the different queues on the basis of a suitable criterion and taking into account the distinct *Quality of Service* (QoS) requirements. The IP packets deriving from the different applications are fragmented in transport blocks that are inserted in the appropriate MAC queues for scheduling actions.

In our scheduler implementation we have made the simplifying assumption, that only one UE can be scheduled (i.e., uses resources) per TTI. Moreover, we only consider video streaming and Web traffic classes. For each application we have the traffic generated at the IP level. Each IP-video packet has a deadline of 150 ms: if an IP-video packet cannot be completely transmitted within this deadline, it is dropped and lost. We have also considered a 'virtual' deadline for IP-Web packets of 500 ms; such deadline only indicates a maximum preferred delay for Web traffic (an IP-Web packet exceeding this deadline is anyway transmitted).

We have considered three alternative scheduling schemes: *Proportional Fairness* (PF) [11], *Earliest Deadline First* (EDF) and *Proportional Fairness with Exponential Rule* (PF-ER) [12].

A. PF Scheduler

PF serves the UE with the largest *Relative Channel Quality Indicator* (RCQI), which represents the ratio between the maximum data rate currently supported by the UE (according to its CQI and the corresponding transport block size) and the UE throughput averaged on a sliding window of suitable width. This approach allows a tradeoff in the service between the UEs that have better channel conditions and those that up to now have received less resources. RQCI is evaluated as:

$$RCQI_k[n] = \frac{R_k[n]}{T_k[n]} \tag{1}$$

where k is the UE index and n = 1, 2, ... is related to the time measured in TTI units. Moreover, $R_k[n]$ is the maximum bit-rate supported by the $k-th$ UE in the next TTI ($R_k[n]$ is calculated as the throughput that is allowed by the CQI in the next TTI interval); $T_k[n]$ represents the average throughput for the $k-th$ UE obtained up to the present TTI.

In particular, referring to the adopted GOOD/BAD channel model, we have:

$$R_k[n] = \begin{cases} 3319 \ \left[\frac{\text{bit}}{\text{TTI}}\right] = 1.6 \text{ Mbit/s} \ \text{(BAD)} \\ \\ 14411 \ \left[\frac{\text{bit}}{\text{TTI}}\right] = 7.2 \text{ Mbit/s} \ \text{(GOOD)}. \end{cases} \tag{2}$$

The limit of the PF scheduler is that it does not provide any QoS differentiation among traffic classes.

B. EDF Scheduler

In the EDF scheduler, packet deadlines are considered so that the packet with the shortest residual lifetime has the highest priority to be transmitted. To implement the EDF

scheme, we have considered that the priority index for the generic $k-th$ UE at the current $n-th$ TTI interval, $P_k[n]$, is given by the ratio between the transmission delay of its oldest IP packet, $d_k[n]$, and the packet deadline, $T_{deadline_k}$ as follows:

$$P_k[n] = \frac{d_k[n]}{T_{deadline_k}} \quad (3)$$

where $T_{deadline_k}$ = 150 ms for an IP-video packet and $T_{deadline_k}$ = 500 ms for an IP-Web packet.

The EDF scheduler could degrade the video performance since the decision of the users to be prioritized does not take into account the available capacity at the physical layer.

C. PF-ER Scheduler

Since the PF scheduler does not differentiate among different traffic types, we have considered here also the PF scheme with the variant of the *Exponential Rule* (ER) [12], where the RCQI index is modified by introducing a multiplicative coefficient as follows:

$$ER_k[n] = \mathrm{RCQI_k}[n] \times a_k e^{\frac{a_k w_k[n] - \overline{aw}}{1+\sqrt{\overline{aw}}}} \quad (4)$$

where:

$$a_k = \frac{-\log(\delta_k)}{T_{deadline_k}} \quad (5)$$

$$\overline{aw} = \frac{1}{N_u}\sum_{k=1}^{N_u} a_k w_k[n]. \quad (6)$$

In (4) and (6), $w_k[n]$ represents the delay (in seconds) of the head-of-line IP-packet of the $k-th$ UE; in (5), δ_k is the desired probability to fulfil the deadline $T_{deadline_k}$ (in seconds); in (6), N_u denotes the total number of UEs in the system.

IV. Comparison of Scheduling Schemes

This Section provides simulations results to compare different scheduling schemes. A first set of results is obtained considering only video traffic provided by real QCIF or SIF video traces. Then, other results are obtained in the presence of simulated video and Web traffic flows.

As for the video traffic traces, we have considered two typical UMTS video streaming scenarios [2]: (*i*) the "cell-phone" scenario with QCIF resolution and a mean bit-rate of 44 kbit/s (7.5 frames/s); (*ii*) the "PDA" scenario with SIF resolution and a mean bit-rate of 160 kbit/s (7.5 frames/s). In both cases video frames are generated and fragmented in IP packets with maximum length of 790 bytes (this is the best tradeoff between RTP/UDP/IP overhead, end-to-end latency [13] and busty error characteristics at the link layer [8]). We have generated video streams of 5000 s in the H.263 formats by means of Quicktime 7.0; the resulting stream has been analyzed to extract the information of the IP datagrams produced by the different video frames. These traffic traces have been transmitted via S-HSDPA by means of the proposed scheduling techniques. We have been able to account for the IP-video packets lost due to both deadline expiration and channel errors. Let $P_{loss,tot}$ denote the total IP packet loss rate for video sources due to both the above phenomena. With current video codecs, the maximum $P_{loss,tot}$ value for guaranteeing an acceptable video quality is around 7%.

Fig. 2 compares EDF and PF schemes as a function of the number of video traffic flows per cell, considering real QCIF traffic traces. We can note that $P_{loss,tot}$ sharply increases with the number of video sources. This is due to the fact that each QCIF-resolution video source produces a very low traffic and, hence, the transport blocks are partly utilized in both the BAD case and the GOOD one. As a consequence, the PF scheme, scheduling traffic accounting for the different channel conditions, is inefficient with respect to the EDF technique that prioritizes the traffic flows on the basis of the remaining lifetime.

Fig. 3 compares EDF and PF schemes as a function of the number of video traffic flows per cell, considering real SIF traffic traces. In this case, the video sources produce a heavier traffic and the PF scheme permits to achieve a better $P_{loss,tot}$ performance and such advantage increases with the traffic load in the system.

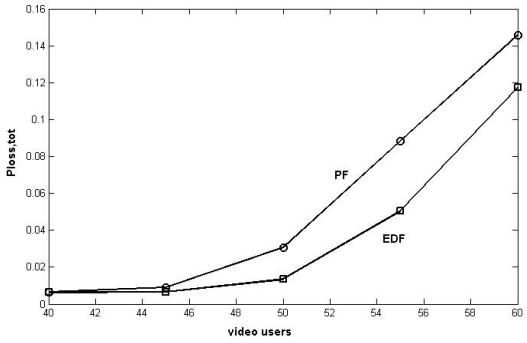

Fig. 2. $P_{loss,tot}$ for IP-video packets (QCIF resolution at 44 kbit/s) as a function of the number of video UEs.

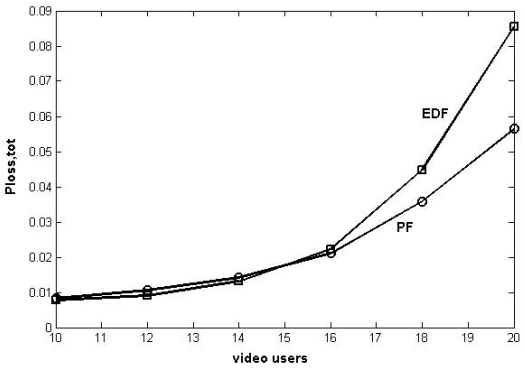

Fig. 3. $P_{loss,tot}$ for IP-video packets (SIF resolution at 160 kbit/s) as a function of the number of video UEs.

In order to compare the scheduling schemes in the presence of different traffic types, we have made simulations with video and Web traffic flows. In this case, we have considered a simulated video traffic according to the Markovian model

in [14] with fitted parameters to the QCIF-resolution traffic traces. Also the Web traffic has been simulated by means the model shown in [15]. In particular, a Web traffic source oscillates between a *packet call* state and a *reading time* one. In the packet call state, a source produces a number of datagrams geometrically distributed with mean value 25 and the datagram interarrival time is exponentially distributed with mean value 0.5 s. In the reading time state (length exponentially distributed with mean value of 4 s) no traffic is generated. Each datagram has a length in bytes with Pareto distribution and mean value 479 bytes. The resulting mean bit-rate produced by a Web traffic source is 5.8 kbit/s.

In Fig. 4, we have shown $P_{loss,tot}$ simulation results for IP-video packets for the PF-ER scheme as a function of parameter δ_k for video users in a case with 20 video sources at a mean bit-rate of 160 kbit/s and 100 Web sources. For Web sources we used a fixed δ_k value equal to 0.5 to guarantee a low prioritization level with respect to video flows. Fig. 4 also shows the $P_{loss,tot}$ values attained by EDF and PF; these are constant values, since they do not depend on δ_k. Fig. 4 clearly proves that the PF-ER scheme achieves the lowest $P_{loss,tot}$ value for IP-video packets, thus allowing a good quality for the video streaming application. As expected, $P_{loss,tot}$ increases with δ_k with PF-ER. Finally, we can see that PF and EDF have unacceptable high $P_{loss,tot}$ values for IP-video packets.

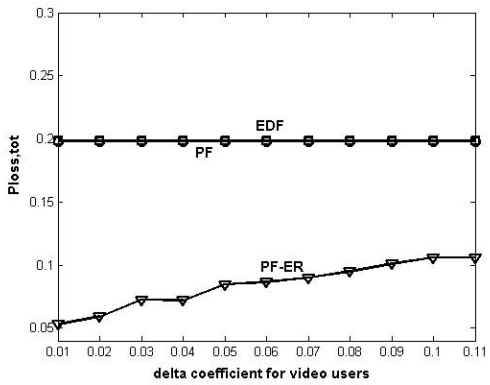

Fig. 4. $P_{loss,tot}$ for IP-video packets with 20 video sources (160 kbit/s mean rate) and 100 Web sources (5.8 kbit/s mean rate).

V. Video Traffic Quality Estimation

Considering only video traffic obtained from the traces (either QCIF or SIF resolutions) we have compared the resulting video quality that we obtain at the application level for the video traffic traces transmitted through the S-HSDPA air interace by means of either PF or EDF[1]. The received video streams, that are affected by packet losses due to deadline expirations and channel errors, have been played again to measure the resulting video quality in terms of *Peak Signal-to-Noise Ratio* (PSNR):

[1]Note that in the presence of the only video traffic class, EDF becomes equivalent to the trivial FIFO case and PF is quite close to PF-ER that also takes into account the residual packet lifetime.

$$PSNR = 10 \times \log_{10} \frac{255^2}{MSE} \quad (7)$$

$$MSE = \frac{1}{w \times h} \sum_{i=1}^{w} \sum_{j=1}^{h} [Orig(i,j) - Deg(i,j)]^2 \quad (8)$$

where $Orig(i,j)$ denotes the original value of the $(i,\ j)$ pixel and $Deg(i,j)$ is the received value of the $(i,\ j)$ pixel for a given video frame.

PSNR has been evaluated for each video frame both in the presence of EDF and PF. The obtained results are described below distinguishing between the two scenarios under consideration.

A. Cell-phone Scenario Results

In this study, the PSNR values have been clipped to 92.17 dB, in case of error-free frame in error-prone channel. This PSNR clipping value corresponds to one error in one color in one frame resolution. Such clipping has been used, because we wanted to avoid infinity PSNR values resulting for zero MSE in (8). The PSNR values for single frames of the investigated sequences have been visualized like empirical histograms. This visualization allows us to see the distribution of visible and invisible impairments.

According to our empirical experiences we set the threshold between visible and invisible impairments at PSNR = 36 dB. We have assumed that the frame degradations higher than 36 dB are almost invisible for human visual systems. Figs. 5 and 6 show the PSNR distribution obtained respectively with the EDF scheme and the PF one in the presence of 40 concurrent video sources (QCIF resolution, mean bit-rate of 44 kbit/s). We have obtained that with PF there are 27.34% less visible impairments (behind 36 dB threshold) with respect to EDF and that almost 85% of frames are error-free (see Table I).

B. PDA Scenario Results

In this case, the PSNR values have been clipped to 96.98 dB, in case of error-free frame in error-prone channel. This PSNR clipping value corresponds to one error in one color in one frame resolution. Figs. 7 and 8 show the PSNR distribution obtained with EDF and PF in the presence of 18 video sources (SIF resolution, mean bit-rate of 160 kbit/s). The mean PSNR value for the whole sequence with PF increases of 3.07 dB with respect to EDF. Moreover, with PF there are 28.51% less visible impairments (behind 36 dB threshold) with respect to EDF and almost 60% of frames are error-free. The achieved results clearly shows that the PF scheduling method has a positive impact on S-HSDPA video streaming services (see Table I).

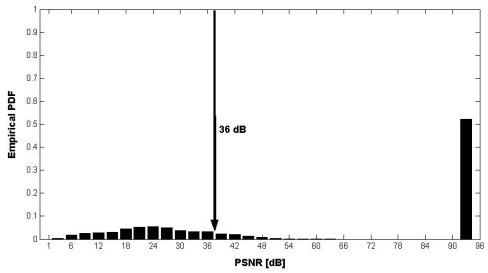

Fig. 5. The empirical PSNR distribution for the cell-phone scenario (QCIF) with EDF scheduling.

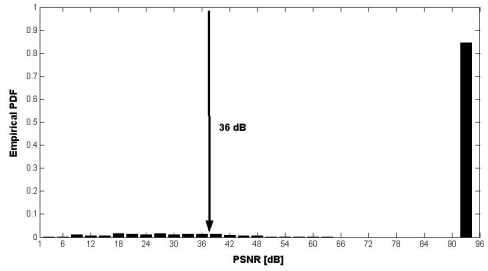

Fig. 6. The empirical PSNR distribution for the cell-phone scenario (QCIF) with PF scheduling.

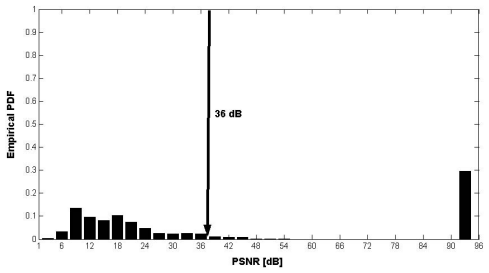

Fig. 7. The empirical PSNR distribution for the PDA scenario (SIF) with EDF scheduling.

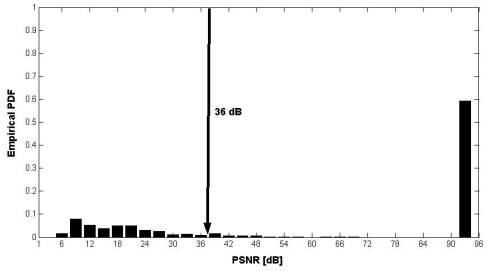

Fig. 8. The empirical PSNR distribution for the PDA scenario (SIF) with PF scheduling.

TABLE I

VIDEO QUALITY RESULTS AND COMPARISONS.

	EDF		**PF**	
Scenario	Cell-phone	PDA	Cell-phone	PDA
$P_{loss,tot}$ [%]	1%	4.5%	1%	3.5%
Mean PSNR [dB]	89.723	92.067	88.67	95.074
Error-free frames [%]	52.19	29.59	84.57	59.14

VI. CONCLUSIONS

This paper has investigated the extension of the terrestrial HSDPA to a GEO-based satellite network to provide broadband multimedia applications to mobile users. The achieved results clearly show the importance of the appropriate selection of the MAC-hs scheduler for S-HSPDA according to a cross-layer approach and optimization that takes into account the actual quality at the application level of the video stream. Further work is needed to characterize the channel model and the interference and, consequently, to define the performance of the physical layer in a more realistic scenario.

ACKNOWLEDGMENTS

This work has been carried out within the European-funded network of excellence SatNEx II (contract No. IST-027393). The contribution of the Institute of Communications and Radio Frequency Engineering to this paper was carried out in cooperation with mobilkom austria AG&Co KG. The views expressed in this paper are those of the authors and do not necessarily reflect those within mobilkom austria AG&Co KG.

REFERENCES

[1] 3GPP, "End-to-end transparent streaming service; Protocols and codecs", TS 26.234.

[2] M. Ries, O. Nemethova, M. Rupp, "Reference-Free Video Quality Metric for Mobile Streaming Applications", *Proc. of the DSPCS 05 & WITSP 05*, pp. 98-103, Sunshine Coast, Australia, December 2005.

[3] 3GPP, "End-to-end transparent streaming service; General description", TS 26.233.

[4] O. Nemethova, M. Ries, M. Zavodsky, M. Rupp, "PSNR-Based Estimation of Subjective Time-Variant Video Quality for Mobiles", *to appear on Proc. of the MESAQUIN*, Prague, Czech Republic, June 2006.

[5] 3GPP, "High Speed Downlink Packet Access; Overall UTRAN Description", R 25.855, Release 5.

[6] H. Holma and A. Toskala, *WCDMA for UMTS: Radio Access for Third Generation Mobile Communications.* Second edition, John Willey & Sons Ltd, 2002.

[7] T. E. Kolding, K. I. Pedersen, J. Wigard, F. Frederiksen, P. E. Mogensen, "High Speed Downlink Packet Access: WCDMA Evolution", *IEEE Vehicular Technology Society News*, Vol. 50, No. 1, pp. 4-10, February 2003.

[8] E. Lutz, D. Cygan, M. Dippold, F. Dolainsky, W. Papke, "The Land Mobile Satellite Communication and Recording, Statistics and Channel Model", *IEEE Trans. Veh. Tech.*, Vol.40, pp.375-386, May 1991.

[9] 3GPP, "Physical layer procedure (FDD)", TS 25.214 v6.3.0 (2004-09).

[10] 3GPP, "UE Radio Access capabilities", TS 25.306 v6.2.0 (2004-06).

[11] T. Kolding, "Link and System Performances Aspects of Proportional Fair Scheduling in WCDMA/HSDPA", *Proc. of the IEEE VTC-Fall 2003*, 4-9 October, 2003, Orlando, Florida, USA.

[12] J. T. Entrambasaguas, M. C. Aguayo-Torres, G. Gomez, J. F. Paris, "Multiuser capacity and fairness evaluation of channel/QoS aware multiplexing algorithms", 4th COST 290 MCM, Wurzburg, October 13-14, 2005.

[13] 3GPP, "Transparent end-to-end Packet Switched Streaming Service (PSS)", TR 26.937.

[14] O. Casals, C. Blondia, "Performance Analysis of Statistical Multiplexing of VBR Sources", *Proc. of INFOCOM'92*, pp. 828-838, 1992.

[15] A. H. Aghvami, A. E. Brand, "Multidimensional PRMA with Priorized Bayesan Broadcast", *IEEE Transactions on Vehicular Technology*, Vol. 47, pp. 1148-1161, 1998.